

Multiscale Simulation of Loading and Electrical Resistance in Silicon Nanoindentation

G. S. Smith, E. B. Tadmor,* and Efthimios Kaxiras

Department of Physics and Division of Engineering and Applied Sciences, Harvard University, Cambridge, Massachusetts 02138
(Received 1 September 1999)

Nanoindentation experiments are an excellent probe of micromechanical properties, but their interpretation is complicated by their multiscale nature. We report simulations of silicon nanoindentation, based on an extended version of the local quasicontinuum model, capable of handling complex Bravais crystals. Our simulations reproduce the experimental load vs displacement curves and provide microscopic information such as the distribution of transformed metallic phases of silicon underneath the indenter. This information is linked to the macroscopic electrical resistance, giving a satisfactory explanation of experimental results.

PACS numbers: 81.70.Bt, 62.20.Fe, 64.70.Kb, 72.20.-i

Nanoindentation experiments have proven very useful in probing the mechanical and high pressure behavior of small samples. This technique has been widely used, for example, to measure the moduli and hardness of thin films [1]. However, a nanoindentation experiment is very complicated due to the large stresses generated near the indenter: defect creation, cracking, and phase transformations may occur. In particular, resistance measurements [2–4] and load vs displacement curves [3,5–7] have provided evidence that reversible phase transformations are common during silicon nanoindentation experiments. The complexity of the phenomena involved in these experiments poses a unique challenge to theoretical analysis. Theoretical models that could provide a comprehensive description of these observations are not available at present. Both atomistic [8] and continuum models [9] have been brought to bear on silicon nanoindentation, but no load vs resistance curves have been produced, while the simulated load vs displacement curves do not capture important features of experimental curves, such as steps [5–7] or hysteretic loops [3]. The computationally intensive nature of atomistic simulations of these phenomena restricts the simulation cell to a size which is many orders of magnitude smaller than the typical size of the solid in an experiment. At the other extreme of the simulation, continuum finite element approaches rely on simple phenomenological constitutive models; a constitutive model for silicon that includes the possibility of phase transformations requires linking the macroscopic strains to the complicated energy landscape associated with microscopic structural changes.

Here we seek to apply a finite element approach free of empirical input (beyond that incorporated in the interatomic potential) to silicon nanoindentation, and compare our results with available experimental data. In particular, we use the local quasicontinuum method [10], a finite element formulation that uses an atomic energy functional to determine the energetics and forces [11], which we have generalized to handle complex Bravais lattices [12]. The method naturally includes nonlinear elastic effects, crystalline anisotropy, and possible uniform structural phase transformations. At the same time, since

the method is based on a finite element framework, it can simulate rather large systems of sizes of order microns; as such it qualifies as a true multiscale approach. In the present simulations we use the Stillinger-Weber (SW) empirical potential to model the interactions at the atomic level [13]. We explored how different potentials affect the results of the simulation, and found that the *macroscopic* measures (such as load vs displacement curves) and the shape of the transformed regions are independent of potential; this is not the case for the specific phases that appear in the indented region. For this study, the exact form of the empirical potential is not crucial; the aim is to ensure that the essential physics of the system is incorporated into the simulation. This includes the rapidly varying strain fields caused by the indenter, the strong elastic coupling between neighboring regions of the material, and a local energy landscape which broadly captures the complexity of the actual solid.

To model nanoindentation, we use a three-dimensional mesh that has a total of 26 640 constant-strain finite elements. The mesh is finest in the vicinity of the indenter, and coarser farther away. The indenter is modeled as a frictionless spherical force field [14]; for the results presented here, the smallest finite element size is 1/9 of the indenter radius. The boundaries of the mesh are about ten indenter radii away from the indenter. Fixed boundary conditions are imposed on the bottom of the mesh, periodic boundary conditions are imposed on the sides, and the top surface is free. The simulation proceeds by gradually lowering the center of the indenter toward the crystal surface and performing zero-temperature minimization of the total energy at each step. At a critical load, finite elements underneath the indenter begin spontaneously transforming from the semiconducting diamond structure to metallic phases of silicon.

We compare first the simulated and experimental load vs displacement curves for a spherical indenter shown in Fig. 1 (the simulation contains no absolute length scale, so results are scaled by the indenter radius, r_I). These are low-load indentations, where unloading begins soon after transformed phases first appear underneath the indenter. In

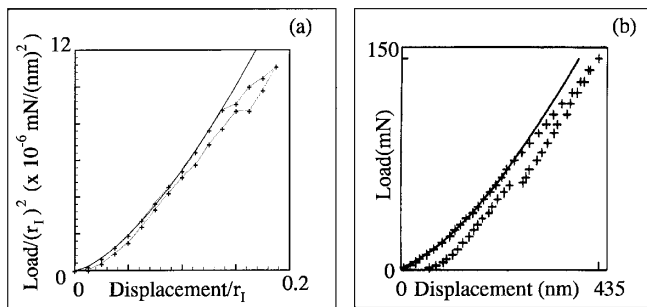


FIG. 1. A comparison of the load vs displacement curves for indentation on the (100) surface of Si: (a) simulation; (b) experiment (from Ref. [5]). The solid lines are fits to the elastic solution.

both curves, upon initial loading there is an elastic regime, where the load varies as the $3/2$ power of the indentation depth [15], as indicated by the solid lines. Deviation from elastic behavior occurs at higher loads, as phase transformations begin to occur underneath the indenter. Finally, both curves exhibit a step in the unloading part, followed by a smooth decline to an unloaded state with residual plastic deformation. In the simulation, this residual deformation is due to finite elements that remain in a metallic phase.

There are some differences in the behavior of the simulated and experimental systems. The experimental curve is for an indenter of radius $8.5 \mu\text{m}$; when the simulation is scaled to this indenter radius the initial transformation occurs at a displacement of 1200 nm , significantly deeper than in experiment. Another difference is that in experiment the phases observed to form underneath the indenter are $\beta\text{-Sn}$ upon loading, and the more complex phases bc8, r8, and hexagonal diamond upon unloading [5–7]. Figure 2 indicates that in the simulation the observed phases are bct5, a fivefold coordinated metallic form of silicon [16], and the simple cubic phase, which forms in small amounts toward the end of the unloading cycle. These discrepancies between simulation and experiment can be attributed to shortcomings in the SW potential, and to the

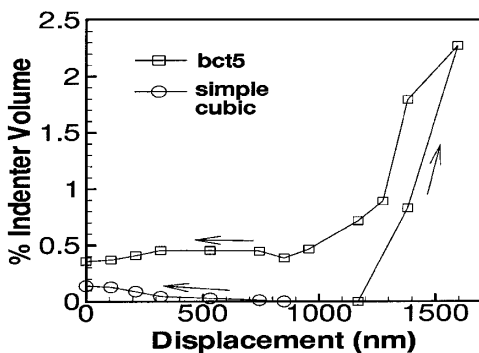


FIG. 2. Amount of transformed phases as a function of indentation depth, expressed as a percentage of the total volume of the spherical indenter.

restriction to a two-atom unit cell in the simulations. The latter choice is made for simplicity, and can be relaxed in future simulations. It is interesting that despite these differences the simulation faithfully reproduces the qualitative features of the experimental load vs displacement curve, including the step upon unloading. In interpreting their experimental results, Weppelmann *et al.* assumed that at this step in the unloading curve one phase transforms into another completely [5,6]. Our results indicate that although the step is associated with a large phase transformation, the number of transformed finite elements continues to change throughout the unloading part of the simulation.

To analyze the simulations, we define a “cluster” as a group of metallic-phase elements, each of which is connected to another element of the group by at least one finite element face. The geometry of the clusters of metallic-phase elements changes dramatically during the course of a load/unload cycle. When fully loaded, a single, well-connected, hemispherical cluster containing nearly all ($>97\%$) of the transformed elements forms underneath the indenter. Upon unloading the transformed elements break into several small clusters, the largest of which contains less than half of the transformed elements. In addition, when the system is unloaded, each remaining cluster becomes tenuously connected.

To investigate the resistance measurements made during indentation experiments, we develop a simple model that uses the simulation results to estimate the resistance. Two types of resistance experiments have been performed [4], shown schematically in Fig. 3. In both, two electrodes are placed on the surface of the silicon sample, and a voltage difference is applied between them. In one experiment, the indenter is directly on top of one of the electrodes; in the other, the indenter is between the two electrodes, slightly offset towards the negative one.

In both experiments, indentation and the resultant metallization underneath the indenter reduces the resistance from the background (R_b) to the measured (R_m) value. The resistance at each of the electrodes is determined by the Schottky barrier that forms at the metal-semiconductor interface [4], and the spreading resistance [17]. These are properties local to each electrode, so we consider the resistances of the positive and negative electrodes to add in series: $R_b = R_b^{(+)} + R_b^{(-)}$. For clusters of metallic-phase

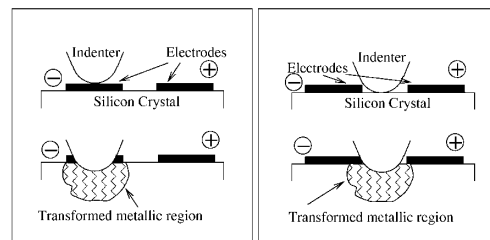


FIG. 3. Schematic of experimental setup for indenting on and between electrodes.

elements that form during indentation and touch an electrode, we take the spreading resistance of a transformed region, R_t , to be in parallel with the electrode's background resistance. This is a reasonable approximation. Current that completes the circuit via the background network will not be significantly perturbed by the indented region, whose dimensions are extremely small compared to the size of the electrode network (see Fig. 2 in Ref. [4]); conversely, the resistance experienced by the current that passes through the indentation region will depend primarily on the local geometry of the transformed region. In the simulation metallic clusters are roughly hemispherical; for such a geometry (neglecting the influence of the electrode network) the spreading resistance for the transformed region of radius a is $R_t \approx \rho/2\pi a$, where ρ is the resistivity of silicon [17]. At each electrode, there is a crossover size $a_c^{(\pm)} \approx \rho/2\pi R_b^{(\pm)}$, determined by the condition $R_b^{(\pm)} = R_t^{(\pm)}$. Using the expression for $a_c^{(\pm)}$, the measured resistance is

$$R_m = R_b^{(-)} \left[1 + \frac{a^{(-)}}{a_c^{(-)}} \right]^{-1} + R_b^{(+)} \left[1 + \frac{a^{(+)}}{a_c^{(+)}} \right]^{-1} \quad (1)$$

and is zero when a transformed region touches both electrodes simultaneously, which corresponds to a short circuit. Here $a^{(\pm)}$ denotes the size of the largest cluster of metallic-phase elements in contact with the corresponding electrode. As our definition of what constitutes a conducting cluster, we assume that only metallic elements fully surrounded by other metallic elements conduct.

First we consider low-load spherical indentations directly on the negative electrode, using the simulation data that produced Fig. 1(a). Simulated load vs resistance curves are shown in Fig. 4. In experiments with the spherical indenter, the silicon sample had a resistivity $\rho \approx 0.05 \Omega \text{ cm}$ [5], but no data were given for the background resistance. To cover the widest range of reasonable R_b values, we plot curves for values of a_c/r_I ranging from 1.8 down to 0.0018, where r_I is the indenter radius; the highest value of a_c/r_I corresponds to a value $R_b^{(-)} \approx 5 \Omega$, and the smallest to $R_b^{(-)} \approx 5000 \Omega$. The predicted behavior could be checked by experiments where the indenter radius is varied; such experiments would shed light on the nature of the reverse transformation upon unloading. In the simulations, where the large metallic cluster at the maximum load gradually fragments and partially transforms back to the diamond phase upon unloading, the resistivity increases smoothly during unloading, especially for the midrange values of a_c/r_I . If the entire transformation were to occur at the step in the load vs displacement curve in Fig. 1, as surmised by Weppelmann *et al.* [5,6], during unloading the resistance would be constant except for a sudden change at the step.

Next we consider deeper simulated indentations. These results are qualitatively different than high-load experiments using spherical indenters [6] presumably because

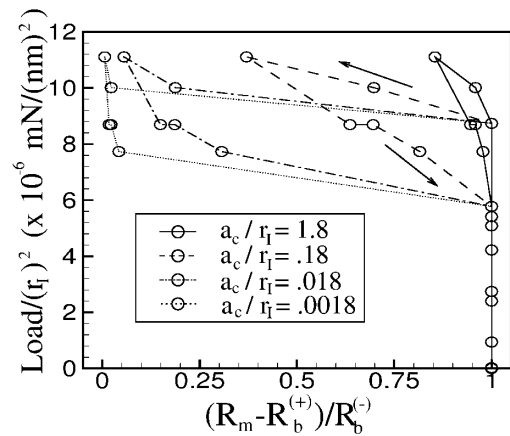


FIG. 4. Load vs resistance curves for indentation on an electrode with an indenter of radius r_I , for different values of a_c/r_I . The maximum indentation depth is $0.19r_I$.

significant cracking is observed in the experiments, while the formation of cracks was not included in the present simulations. However, the simulation results are similar to the low-load Berkovich indenter load vs displacement curves [3,4], where cracking does not occur. In particular, both have a reproducible hysteresis loop, as shown in Fig. 5. The same experiments also provide load vs resistance measurements [4]. These results present a further opportunity to test the validity of the simulation and the simple electrical model presented above. To compare the simulated load vs resistance curves with the experimental curves we use the experimentally determined values for the constants in Eq. (1): $\rho \approx 10 \Omega \text{ cm}$, $R_b^{(+)} \approx 5 \text{ k}\Omega$. The total background resistance R_b varies from one experiment to the next; $R_b^{(-)}$ is chosen to ensure that $R_b = R_b^{(+)} + R_b^{(-)}$ is equal to the experimentally measured total background resistance. With these parameters, $a_c \approx 1 \mu\text{m}$, which is the approximate size of the indentations in the experiments. Had the indentations been significantly smaller, they would not have affected the measured resistance; had they been significantly larger, a smooth change in resistance as a function of indentation depth would have been difficult to observe. Using these constants in Eq. (1), we

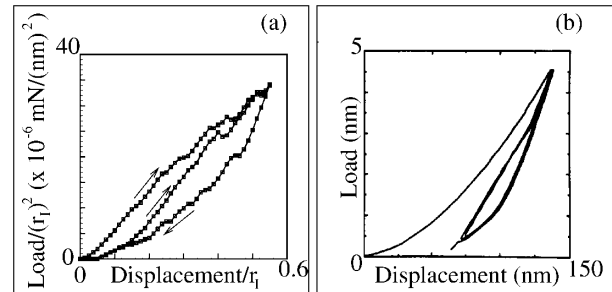


FIG. 5. A comparison of load vs displacement curves: (a) deep indentation simulation; (b) Berkovich indenter experiment (from Ref. [3]).

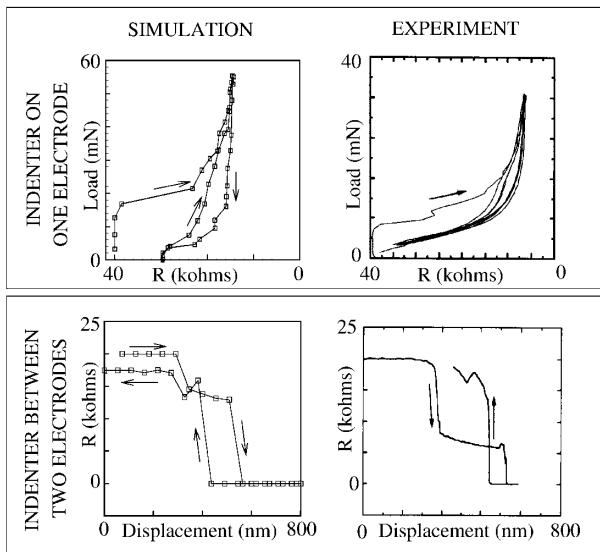


FIG. 6. Comparison of experimental and high-load simulated resistance curves for the two different experimental geometries shown in Fig. 3. The experimental curves are taken from Ref. [4].

obtain the simulated resistance curves shown in Fig. 6. The simulation data were scaled to a maximum indentation depth that matches that of the corresponding experimental curves, also shown in Fig. 6. The simulated curves reproduce well the qualitative features of the experimental results. Given the shortcomings of the Stillinger-Weber potential used in the present calculations, this qualitative agreement suggests that the basic features of the resistance measurements are insensitive to the details of the microscopic energy surface and the indenter geometry in the absence of cracking.

In summary we have used a multiscale approach based on the local quasicontinuum model to simulate resistance and load vs displacement curves for silicon nanoindentation; the results reproduce qualitatively available experimental data. In the course of comparing simulation and experiment we have discussed several open issues and possible future work that would help clarify the behavior of this system. For example, experimental resistance measurements for spherical indenters of varying radii would help determine whether the reverse transformation upon unloading occurs suddenly or gradually. In all simulations we used a spherical indenter, but similarities were noted between the deeper simulated indentation results and Berkovich indenter experiments: further work is needed to understand how factors such as indenter shape and cracking in the indented region influence whether macroscopic curves exhibit a step or reproducible hysteretic loop.

It is a pleasure to acknowledge useful discussions with Michael J. Aziz, Michael Ortiz, Jim Sethna, Frans

A. Spaepen, and Umesh V. Waghmare. Work was supported by the Harvard Materials Research Science and Engineering Center, which is funded through the NSF.

*Present address: Faculty of Mechanical Engineering, Technion-Israel Institute of Technology, 32000 Haifa, Israel.

- [1] Li Xiadong and B. Bhushan, *Thin Solid Films* **340**, 210 (1999); W. C. Oliver and C. J. McHargue, *Thin Solid Films* **161**, 117 (1988).
- [2] D. R. Clarke, M. C. Kroll, P. D. Kirchner, R. F. Cook, and B. J. Hockey, *Phys. Rev. Lett.* **60**, 2156 (1988).
- [3] G. M. Pharr, W. C. Oliver, and D. R. Clarke, *J. Electron. Mater.* **19**, 881 (1990).
- [4] G. M. Pharr, W. C. Oliver, R. F. Cook, P. D. Kirchner, M. C. Kroll, T. R. Dinger, and D. R. Clarke, *J. Mater. Res.* **7**, 961 (1992).
- [5] E. R. Weppelmann, J. S. Field, and M. V. Swain, *J. Mater. Res.* **8**, 830 (1993).
- [6] E. R. Weppelmann, J. S. Field, and M. V. Swain, *J. Mater. Sci.* **30**, 2455 (1995).
- [7] A. Kailer, Y. G. Gogotsi, and K. G. Nickel, *J. Appl. Phys.* **81**, 3057 (1997).
- [8] J. S. Kallman, W. G. Hoover, C. G. Hoover, A. J. De Groot, S. M. Lee, and F. Wooten, *Phys. Rev. B* **47**, 7705 (1993); R. Pérez, M. C. Payne, and A. D. Simpson, *Phys. Rev. Lett.* **75**, 4748 (1995).
- [9] A. K. Bhattacharya and W. D. Nix, *Int. J. Solids Struct.* **24**, 881 (1988); J. A. Knapp, D. M. Follstaedt, S. M. Myers, J. C. Barbour, and T. A. Friedmann, *J. Appl. Phys.* **85**, 1460 (1999).
- [10] In the local quasicontinuum method, interface energies between finite elements are neglected. This sets a minimum length scale for the simulation, above which the strain energy in each finite element volume is much larger than the interfacial energy. Based on our recent unpublished density functional theory calculations, we estimate this length scale to be of the order of 10 nm, which is 2 orders of magnitude smaller than the minimum finite element size in the present simulation; here the length scale is set by comparing with relevant features of experimental setups.
- [11] E. B. Tadmor, M. Ortiz, and R. Phillips, *Philos. Mag. A* **73**, 1529 (1996).
- [12] E. B. Tadmor, G. S. Smith, N. Bernstein, and E. Kaxiras, *Phys. Rev. B* **59**, 235 (1999).
- [13] F. H. Stillinger and T. A. Weber, *Phys. Rev. B*, **31**, 5262 (1985).
- [14] C. L. Kelchner, S. J. Plimpton, and J. C. Hamilton, *Phys. Rev. B*, **58**, 11085 (1998).
- [15] H. Hertz, *J. Reine angewandte Mathematik* **92**, 156 (1882).
- [16] L. L. Boyer, E. Kaxiras, J. L. Feldman, J. Q. Broughton, and M. J. Mehl, *Phys. Rev. Lett* **67**, 715 (1991).
- [17] R. Holm, *Electric Contacts: Theory and Application* (Springer-Verlag, New York, 1967).